Laser Production of Metallic Ultra-Fine Particles

Akira MATSUNAWA*, Seiji KATAYAMA**, Akihiro SUSUKI*** and Tomio ARIYASU****

Abstract

Laser production of various ultra-fine metal and alloy particles was undertaken by repeating pulsed Nd: YAG laser shots on target materials such as commercially pure metals and binary alloys in Argon (Ar) or Helium (He) atmosphere. Especially, the characteristics of morphology, crystal structure, size distribution and color of particles and the influence of ambient pressure on the particle size and distribution were investigated by transmission electron microscope (TEM), its diffraction method and X-ray diffractometer, and the compositions of alloy particles were analyzed by energy dispersive X-ray spectrometer (EDX) of scanning electron microscope (SEM) and compared with those of target alloys.

As a result, ultra-fine metal and alloy particles of less than 40 nm in mean size and less than 150 nm in maximum size could be produced from their target materials by pulsed laser heating-evaporation in Ar or He atmosphere at 0.1 MPa (1 atm). The mean sizes of Fe, Ni and Ti particles became smaller to less than 5 nm with a decrease in the ambient pressure to 0.1 kPa, and consequently it was judged that the particle size and distribution could be easily controlled by regulating ambient pressure. The powder yield was larger for Fe, Ni and Ti than Cu and Al of greater laser reflectance and Mo of higher vaporization temperature as compared at the same laser irradiation conditions. Moreover, laser production of ultra-fine alloy powders was feasible, and their compositions and structures were roughly controllable by selecting the compositions of target alloys.

KEY WORDS: (Lasers) (Ultra-Fine Particles) (Powder Production) (Metals) (Alloys) (Gas Evaporation Process)

1. Introduction

Extremely small particles of less than 1μm in size are generally termed "ultra-fine particles".[1)–3)] Since such fine particles possess excellent physical or chemical properties different from those of bulk materials, they attract attention as promising new high-performance materials for magnetic, electronic and sintering materials, chemical catalysts, sensors, etc.[1)–8)] There are many physical and chemical or dry and wet processes for the production of ultra-fine particles[1)–19)]. An ideal production process should satisfy the following conditions: (1) Particles are stable or preservative, (2) their sizes and size distribution are controllable, (3) their surfaces are clean or controllable, (4) they are easily collected, and (5) their yield is large.[9)] The evaporation techniques in gas atmosphere using heating sources such as laser beam, electron beam, arc plasma, plasma jet, resistance heater and induction heater have been mainly studied as clean means and brought into use.[3)–20)] In particular, high frequency induction heater, plasma jet and active plasma arc processes are commercially employed.[3),6),20)] However, they have a few defects. For example, the induction heater has the difficulty in evaporating high melting point materials and costs a lot.[3),6)] The plasma jet blows away melted materials easily.[7)] The active plasma arc process produces ultra-fine particles of rather larger sizes from most metals and hydride powders from some metals.[6),10)–12)]

On the other hand, there are some papers on laser production processes. Uyeda, et al.[16)] and Kato[17)] reported the results of oxide particles produced from some target oxides by CW CO_2 laser irradiation, and Haggerty, et al.[18),19)] described the formation results of ultra-fine Si particles from SiH_4 excited by CO_2 laser and moreover SiC or Si_3N_4 powders by reacting SiH_4 with C_2H_4 or NH_3. Besides, high power lasers have recently been developed.[21),22)] It is therefore considered that these laser heating-evaporation processes are characterized by the great controllabilities of production conditions. For example, ambient atmosphere, its pressure, evaporated part and energy (or power) density at laser-irradiated part are easily selected and controllable, and moreover the laser irradiation can heat a target material up to the vaporization temperature almost instantaneously.[23)–25)] However, there are few papers dealing with the production of ultra-fine particles from metal plates by utilizing these characteristics of high power lasers.

Therefore, in this study, with the objective of obtaining fundamental data on the laser production of ultra-fine powders, a variety of ultra-fine metal and alloy particles were produced from their pure metals and binary alloys by pulsed YAG laser irradiation in Ar or partly He atmosphere. First, in order to evaluate the laser produc-

† Received on Nov. 7, 1986

* Professor
** Research Instructor
*** Graduate Student of Kansai University
**** Professor of Kansai University
(3-3-35 Yamatechyo, Suita, Osaka 565, JAPAN)

Transactions of JWRI is published by Welding Research Institute of Osaka University, Ibaraki, Osaka 567, Japan

tion process in terms of controllability, we investigated the formation behavior of particles, laser irradiation conditions for particle production and yield of various metal particles. Subsequently, so as to characterize metal and alloy particles, the shape, size distribution and crystal structure of particles were studied by transmission electron microscope (TEM), its electron diffraction and X-ray diffraction method, and furthermore the compositions of alloy powders were analyzed by energy dispersive X-ray spectrometer (EDX) of scanning electron microscope (SEM).

2. Materials and Experimental Procedure

2.1 Materials used

Materials used are commercially available pure metals of Fe, Ni, Ti, Al, Mo, Zr, Cr, Nb, Ta, W, Si, V, Mn, Co, Cu, Ag, Zn, Ge, Sn and Pb, and Ni-Ti, Fe-Ti and Cu-Ni binary alloys (about 20, 40, 55, 65 and 80 wt%Ti for Ni-Ti alloys; 20, 33, 54, 70 and 85 wt%Ti for Fe-Ti alloys; and 20, 40, 60 and 80 wt%Ni for Cu-Ni alloys). The metal sheets are mainly about 25 mm in length, 20 mm in width and 3 mm in thickness ($25^{l} \times 20^{w} \times 3^{t}$mm, for short); and 1^{t}mm for W, Cu and Ag. All target alloys were produced as nuggets (about 5^{t}mm) of about 20g from mixed pure metals in the arc furnace. The compositions of Ni-Ti, Fe-Ti and Cu-Ni alloys were analyzed by the EDX analysis method, and are indicated as NT2, NT4, etc in the binary phase diagrams[26] in **Fig. 1** (a), (b) and (c), respectively. The surfaces of materials were polished with No. 400 emery paper and cleansed by acetone.

2.2 Laser apparatus and irradiation conditions

The pulsed Nd: YAG laser apparatus (Control laser: Model 428, delivering an average power of 200 W at 1.06μm wave length and 3.6 ms pulse width) and atmosphere- and pressure-controllable chamber were utilized for the production of ultra-fine particles, as their schematic outline is shown in **Fig. 2**. The laser with pulse energy of 10 to 33 J/p through the quartz window was irradiated by 130 mm focal-length lens at the defocused distance of 0 to 40 mm on each metal sheet. Laser beam focused was about 0.6 to 3.5 mm in spot diameter, and laser power density was varied in the range of about 3×10^{4} to 6×10^{6} W/cm^{2}.

The production of metal particles was first performed from various pure metals in Ar or He atmosphere at 0.1 MPa (1 atm). Particularly, in order to determine important factors in controlling particle sizes, the influence of laser irradiation conditions or chamber (atmosphere) pressure on the particle size and distribution of ultra-fine particles was investigated in the power density range of

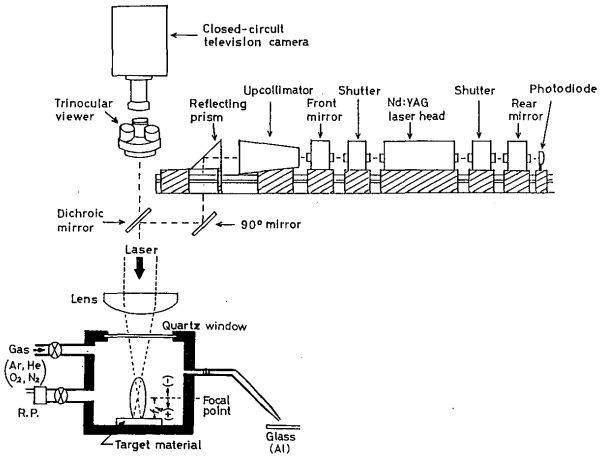

Fig. 2 Schematic configuration of optical components in Nd: YAG laser apparatus and atmosphere- and pressure-controllable chamber for producing ultra-fine particles.

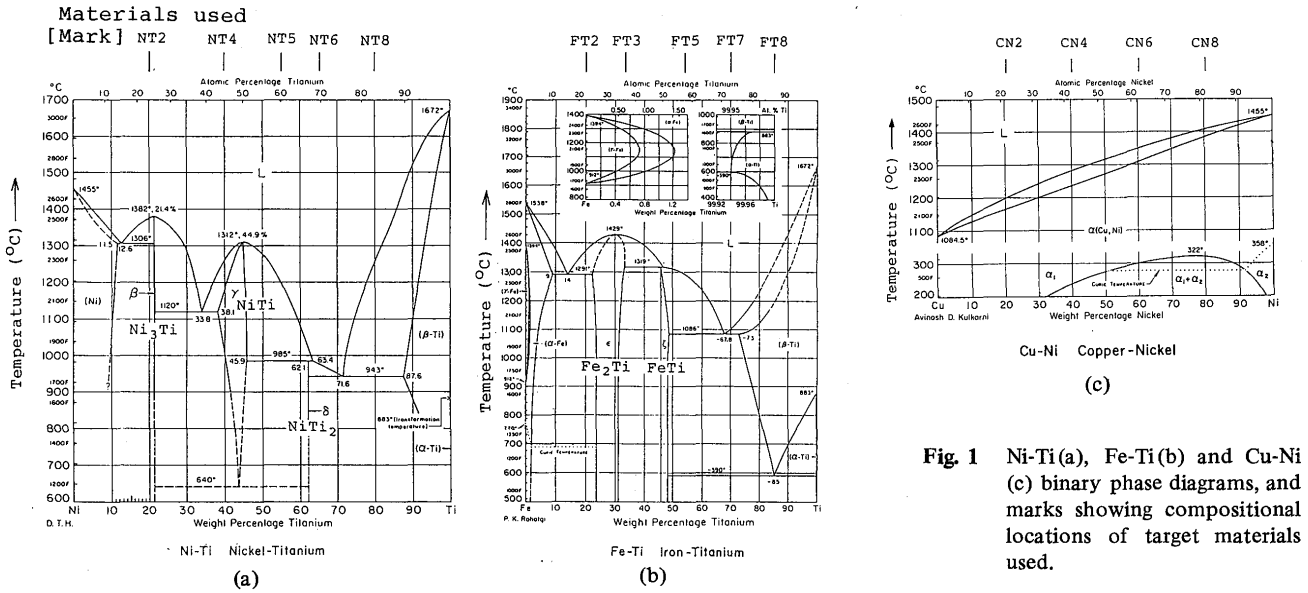

Fig. 1 Ni-Ti(a), Fe-Ti(b) and Cu-Ni (c) binary phase diagrams, and marks showing compositional locations of target materials used.

about 0.9 to 3.1 MW/cm^2 or in the pressure range of 10 Pa (0.1 Torr) to 0.2 MPa (2 atm) by using Fe, Ni and Ti sheets. Subsequently, a formation feasibility of ultra-fine alloy particles was investigated.

2.3 Metallographic examination

Ultra-fine particles were observed and identified by TEM and electron diffraction method using conventional carbon-extraction replices from the collection glass, which was placed about 10 to 50 mm above the target plate or was used by spray method. Their shapes, particle sizes and size distribution were examined. Identification of ultra-fine metal and alloy particles was further carried out by X-ray diffractometer method of powders collected by spray method (see Fig. 2).

2.4 Optical measurements

Three optical measurement methods were conducted to clarify the behavior characteristics of a plume (or luminous body) and ultra-fine particles occurring from the target plate. These schematic optical configurations are shown in **Fig. 3**. Temporal changes in cw He-Ne probe laser beam ($\lambda = 632.817$ nm) intensity, selected plume emission light ($\lambda = 411.27$ nm of TiI) intensity and scattered incident beam ($\lambda = 1.06\mu$m) intensity were measured at a certain height above the target surface, as shown in Fig. 3 (a), (b) and (c). The propagation velocities of vapor and luminous fronts as well as the initiation times, occurrence durations and end times of evaporation and light emission at the target surface were determined by performing the experiment at different heights, as shown in Fig. 3 (d).[23]

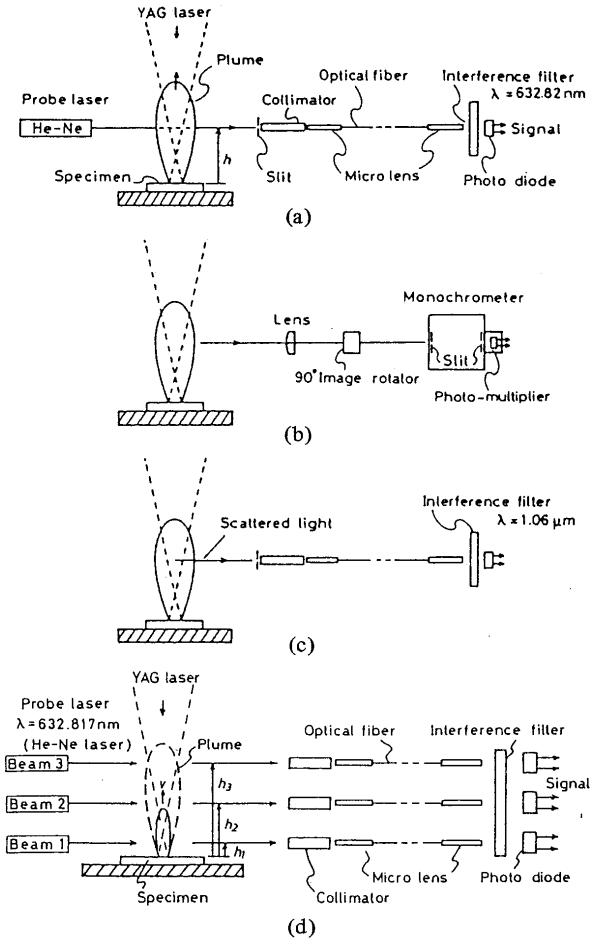

Fig. 3 Schematic illustration of optical measurement arrangements for elucidating properties of vapor plume: (a) cw He-Ne probe laser beam method; (b) monochrometer method; (c) 90° scattered YAG laser intensity measurement; and (d) probe laser beam method at different heights.

3. Results and Discussion

3.1 Evaporation phenomenon and laser irradiation conditions for ultra-fine particle production

3.1.1 Plume and ultra-fine particles

When a pulsed Nd: YAG laser with high power is irradiated on a target plate, a plume (a luminous body) or spattering is observed to occur above the plate surface, depending on the laser energy or power density.[23)–25)] **Figure 4** (a) and (b) are still pictures showing typical examples of plume + spattering and only plume observed over Ti plate exposed to one pulsed laser shot, and the

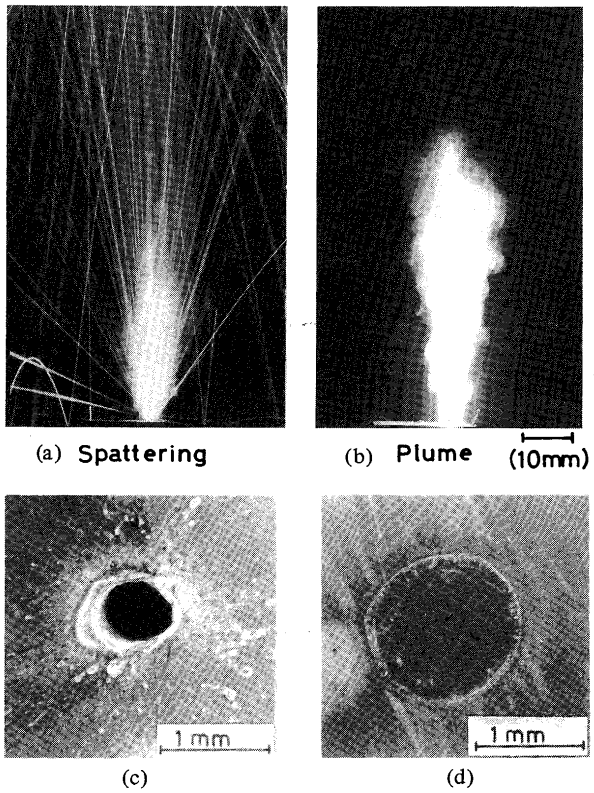

Fig. 4 Spattering + plume (a) and plume (b) induced from Ti surface by laser irradiation, and respective surface appearances of laser-irradiated Ti sheet (c) & (d).

plate surfaces after their respective occurrences are exhibited in SEM photos of Fig. 4 (c) and (d). Generally, in the case of high laser power density, spattering is generated together with plume and a hole or hollow is observed in the laser-irradiated part, as shown in Fig. 4 (a) and (c), while in the case of the lower one, plume is only formed and melted zone is seen after laser shot as indicated in Fig. 4 (b) and (d). The particles produced by the respective laser irradiation conditions were collected on the glass and observed by the TEM. The TEM photos are shown in **Fig. 5**. Some particles of more than 100 nm or 1μm in size were formed in addition to a number of ultra-fine particles under the laser irradiation conditions for the plume + spattering formation. On the other hand, ultra-fine particles of less than 100 nm in size were formed under the conditions for the plume generation. Besides, in the case of much lower laser power density, small or no plume, no melted zone and no evaporated zone are observed and no ultra-fine particles cannot be produced.

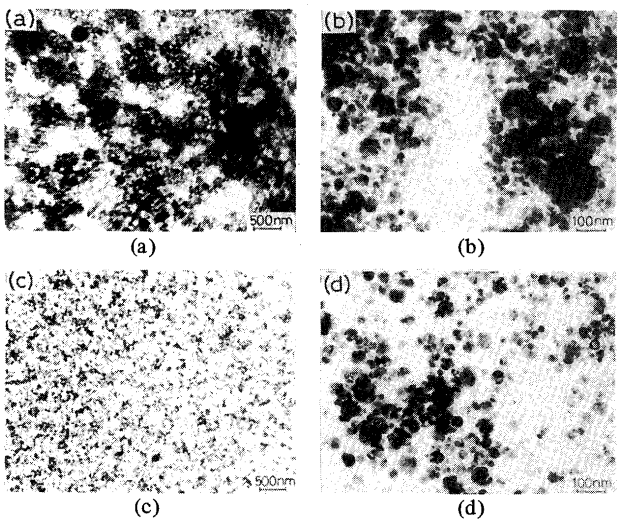

Fig. 5 TEM photos of ultra-fine particles produced from Ti sheet under laser irradiation conditions for formations of spattering & plume ((a) & (b)) and plume ((c) & (d)).

From the above results, it is judged that the laser irradiation conditions for plume formation are preferable to those for plume + spattering generation for the production of ultra-fine particles, because extremely large particles are made in addition to hole formation in the laser irradiated part by spattering for the latter conditions.

Spectroscopic analyses were first made of a plume generating from a pure Ti plate. As a result, strong line spectra of neutral Titanium atoms (TiI), absorption spectra of the resonant TiI, the broadened lines in its neighborhood and weak lines of singly ionized Titanium ions (TiII) were identified in spectral lines of plumes. It was thereby found that the plume generated by pulsed YAG laser shot under normal ambient pressure was not a strongly ionized plasma but a weakly ionized plasma surrounded with atomic vapors of high densities at low temperatures.[23)]

Subsequently, the behaviors of plume and ultra-fine particles under the laser irradiation conditions for the plume generation were investigated using optical measurement methods. The results are shown in **Fig. 6**. Fig. 6 (a) presents the relation between the incident laser output power shape and temporal variations in cw He-Ne probe laser beam intensity, spectral line intensity and scattered

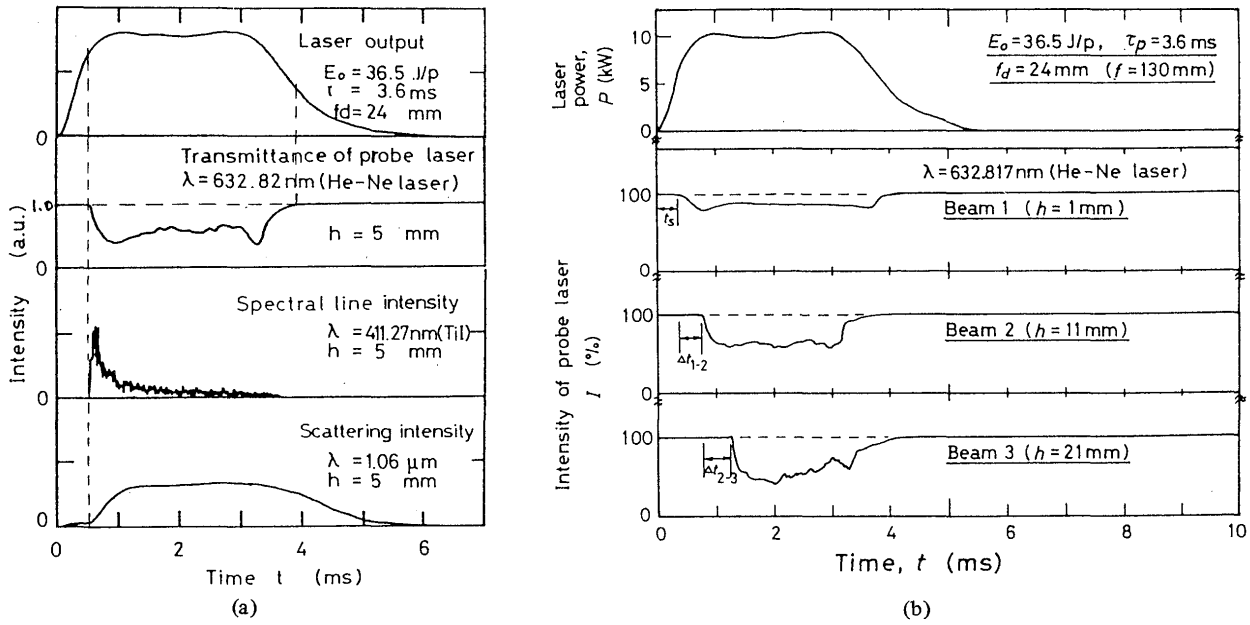

Fig. 6 Various optical characteristics of plume, vapor or particles from target material during pulsed YAG laser irradiation: (a) output power shape of YAG laser, transmittance of He-Ne probe laser, temporal change of spectrum line, and scattering of incident YAG laser beam; and (b) output power shape and cw He-Ne probe laser behavior at different heights.

incident laser beam intensity, and Fig. 6 (b) demonstrates the relationship between the laser output power form and the behavior of cw He-Ne probe laser beams measured at the different heights of 1, 11 and 21 mm above the Ti sheet surface during laser irradiation. The measurement result of spectral line intensity means that the emission of light from a plume is strong for an extremely short time just after the evaporation initiation. Such results obtained at different heights and the observation results of high speed photographs confirmed that the emission of a plume was generated on the plate surface at the initial stage of the laser irradiation and the luminous body was formed on the top part of vapor flow and propagated rapidly upward the plate.[23)–25)] Therefore, the decreases in the probe laser beam intensity and the increase in scattered light intensity are attributed to the flow of non-excited vapors, or ultra-fine particles. For example, from the relation between the difference in the height, $h_2 - h_1$, and the delay time of the intensity variations in probe laser beams, t_{1-2}, as shown in Fig. 6 (b), the growth rate of evaporated particles obtained was about 25 m/s, and accordingly the start time of evaporation was deduced to be approximately 0.34 ms. Such high evaporation rates of particles are beneficial to the production of ultra-fine powders. In addition, since both the decreases in probe laser intensity and the increase in scattered laser beam intensity due to the evaporation are observed almost throughout the laser shooting duration, pulse laser energy is considered to be efficiently consumed for the particle formation.

Furthermore, **Fig. 7** is a still picture of a plume generated from a Ni sheet with 30° declination against the horizontal of the X-Y work table. The plume occurs almost perpendicularly to the sheet surface. This suggests that the collection of ultra-fine particles should be very easy and efficient by setting a collection nozzle or plate over the plume head in this laser process.

Fig. 7 Plume generated from 30° inclination specimen (Ni) by pulsed laser shot.

3.1.2 Laser irradiation conditions and yield of ultra-fine particles

As described in 3.1.1, ultra-fine particles were efficiently produced under the laser irradiation conditions for the plume formation but not for the plume + spattering formation. Therefore, the conditions of one-pulse laser energy and defocused distance at plus side for the plume and plume + spattering formation were investigated on each metal sheet by the laser irradiation in Ar atmosphere at 0.1 MPa. **Figure 8** (a), (b), (c) and (d) show the condition domains of plume and plume + spattering formations for Fe, Ti, Mo and Cu sheets, respectively. For Fe in Fig. 8 (a), plume was easily formed in a wide range of laser irradiation conditions. For Ti, as shown in Fig. 8 (b), the region of plume formation became wider, but for Mo and Cu the regions were narrower, as seen in Fig. 8 (c) and (d), respectively. The regions of laser irradiation conditions for plume formation were narrower in the order of Ti, Zr, Fe, Ni, Cr, Al, Mo and Cu. This means that the laser has difficulty in evaporating the materials of great light-reflectance, high vaporization temperatures and/or great thermal diffusivity.

The evaporated weight losses of each metal were

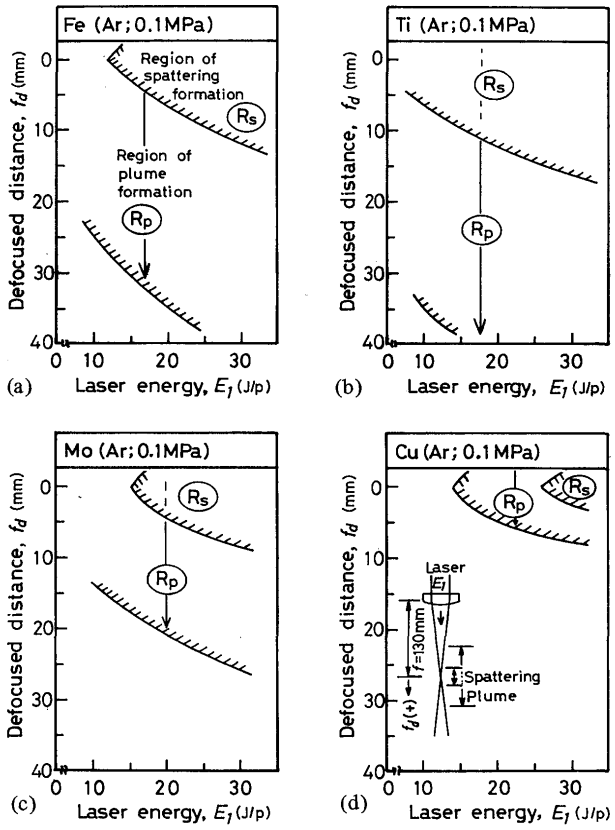

Fig. 8 Laser irradiation condition domains of spattering and plume formation for Fe, Ti, Mo and Cu sheets.

measured and compared as an index of the production yield of particles. It is natural to understand that the evaporated weight loss (particle yield) caused by one laser shot should be dependent upon laser energy, defocused distance, energy density, power density, atmosphere, chamber pressure, target materials, their surface conditions, etc.[25] **Figure 9** indicates the evaporated weight losses of Fe, Ni, Ti, Mo and Al induced by a single laser shot under the same laser energy of 22 J/p in Ar atmosphere at 0.1 MPa. The defocused distances adopted were both 10 mm (15 mm for Ti) and the shorter ones without spattering (depending on each metal; 7 mm for Mo to 14 mm for Ti). By comparison under the same laser irradiation conditions, the evaporated weight losses of Fe, Ni and Ti are about 60 to 90μg, and are several times heavier than those for Al and Mo of 10μg in the weight loss. When the laser irradiation conditions were restricted to the use of the same pulse laser energy, the evaporated weight losses were increased by about 10% for Ti to 3 times for Mo by decreasing the defocused distance or increasing the laser energy (power) density, although the loss for Al still remains small. The evaporated weight loss obtained by one laser shot is about 100μg for Fe and Ni. Consequently, the average evaporation rate of particles is 25 mg/s (0.1 mg/4 ms; 1.5 g/min; 90 g/hr), and the production yield of powders is 3 g for 1 hour, assuming that a laser with the energy of 22 J/p is repeated 8 times per

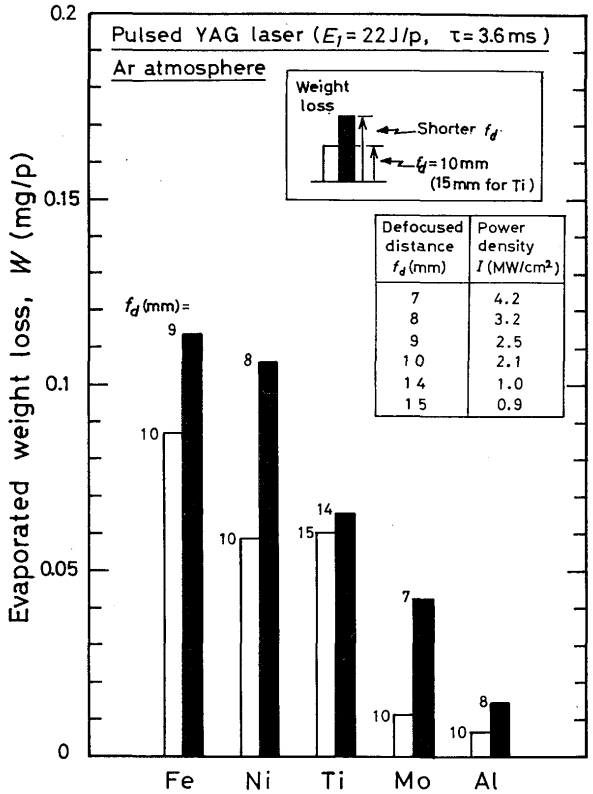

Fig. 9 Evaporated weight losses of Fe, Ni, Ti, Mo and Al caused by single laser shot with 22 J/p under 0.1 MPa Ar atmosphere.

second by using this 200 W laser apparatus. On the other hand, the formation rates of ultra-fine Fe particles produced by the active plasma arc process in Ar-50%H_2 gas and plasma-jet (power: 10 kW) techniques in He-15%H_2 gas are reported to be about 20 mg/s[10)–12)] and 3.3 mg/s[13)], respectively, and the yield of powders produced commercially by the former process can be approximately 50 g. By comparison, the laser process used in this study is characterized by small yield of powders but extremely high formation rate of ultra-fine particles for Fe and Ni. On the other hand, low production yield rate of particles may be the case for the great laser reflectance materials such as Al and Cu and high melting point materials such as Mo.

Taking Ni or SUS 310S stainless steel for instance, the evaporated weight loss was increased by about 1.5 to 2 times by increasing the pulse laser energy by 2 times. Therefore, some considerations taken into account so as to obtain a larger production yield are the utilization of a higher energy (power) laser, the procedure for enhancing the absorption of laser energy such as the use of the plate heated at high temperatures or in the molten state and the usage of powders instead of a plate, the use of such a laser with other processes together, and so on.[25]

3.2 Morphology, crystal structure and particle size distribution of ultra-fine metal particles

3.2.1 Characteristics of various ultra-fine metal particles

Evaporated ultra-fine metal particles were produced from various metals in Ar or He atmosphere at 0.1 MPa (1 atm) by laser shots under the conditions for plume formation, and their morphology, crystal structure and particle size distribution were investigated using TEM and X-ray diffractometer.

Figure 10 (a) and (b) exhibit the TEM photos (at lower and higher magnification, respectively) of particles adhering to the glass sheet placed about 30 mm above the Fe sheet surface after the laser irradiation under the plume formation condition (E_1 = 33 J/p, f_d = 15 mm) in Ar atmosphere, and Fig. 10 (c) and (d) show the electron diffraction rings of particles and particle size distribution, respectively. Fig. 10 (e) indicates the X-ray diffractometer result of ultra-fine powders collected by the spray method. Based upon the analytical results in Fig. 10 (c) and (e), particles were identified as bcc type α-Fe (a_o = 2.867Å). These Fe particles are in the projection shape of mainly polygon or globule, as seen in Fig. 10 (a) and partly oxtagon as shown in Fig. 10 (b). Moreover, they had a tendency to be linked together like chains. About 95% of particles were less than 40 nm in size and the average diameter was approximately 20 nm. Such powders were found to be pretty uniform in size. Fe particles made in He atmosphere showed the same physical characteristics

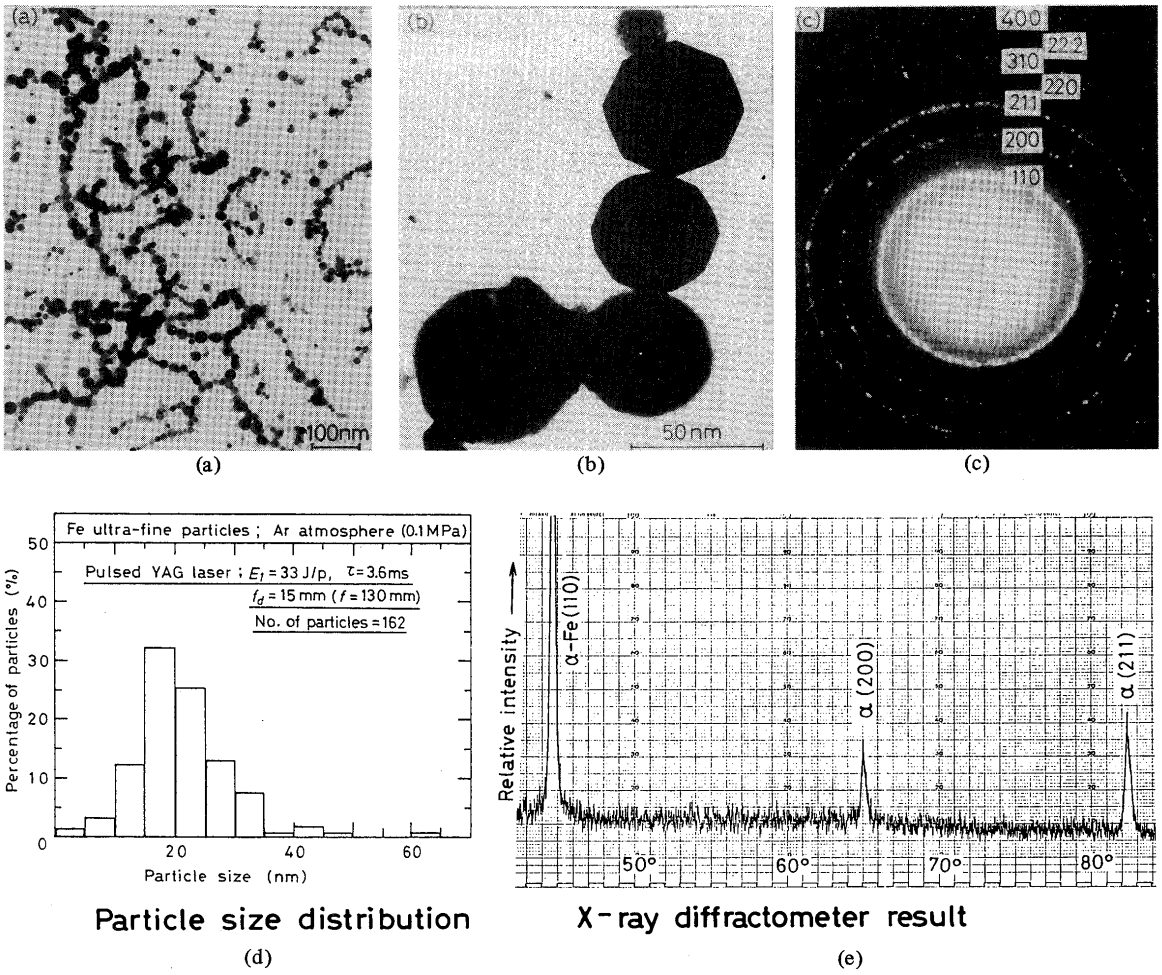

Fig. 10 TEM photos ((a) & (b)), electron diffraction rings (c), particle size distribution (d) and X-ray diffractometer result (e) of ultra-fine Fe particles made by laser heating-evaporation process in Ar atmosphere at 0.1 MPa.

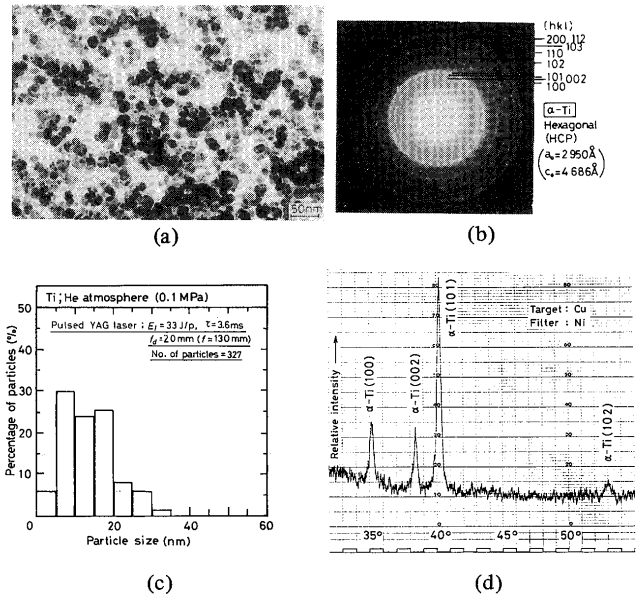

Fig. 11 TEM photo (a), electron diffraction rings (b), particle size distribution (c) and X-ray diffractometer result (d) of ultra-fine Ti particles made by laser heating-evaporation process in He atmosphere at 0.1 MPa.

as those in Ar, but had a smaller average size of 12 nm and narrower particle size distribution than those in Ar.

Figure 11 (a) to (d) show the TEM photo of particles made from a Ti sheet by laser shots in He atmosphere, electron diffraction rings from the particles, particle size distribution and X-ray diffraction result. Ultra-fine particles are spherical in shape in the size range of less than 40 nm, and were identified to be hcp α-Ti phase, which is stable at lower temperatures than 1155 K (882°C). Particles of bcc β-Ti phase, which is stable at higher temperatures of 1155 (882) to 1941K (1668°C), were not detected.

Figure 12 (a) to (f) show the TEM photos of ultra-fine particles produced from Ni, Zr, Nb, Al, Cr and Mo sheets in Ar or He atmosphere at 0.1 MPa. These particles had a size range of less than 70 nm. Most particles are spherical, granular or polygonal in shape, and in particlar Cr and Zr particles are hexagonal or oxtagonal in the projection form (flatten rhombic trisoctahedron). According to analytical results of the electron and X-ray diffractions, respective metallic particles were identified to be Ni (fcc), α-Zr (hcp), Nb (bcc), Al (fcc), α-Cr (bcc) and Mo (bcc)

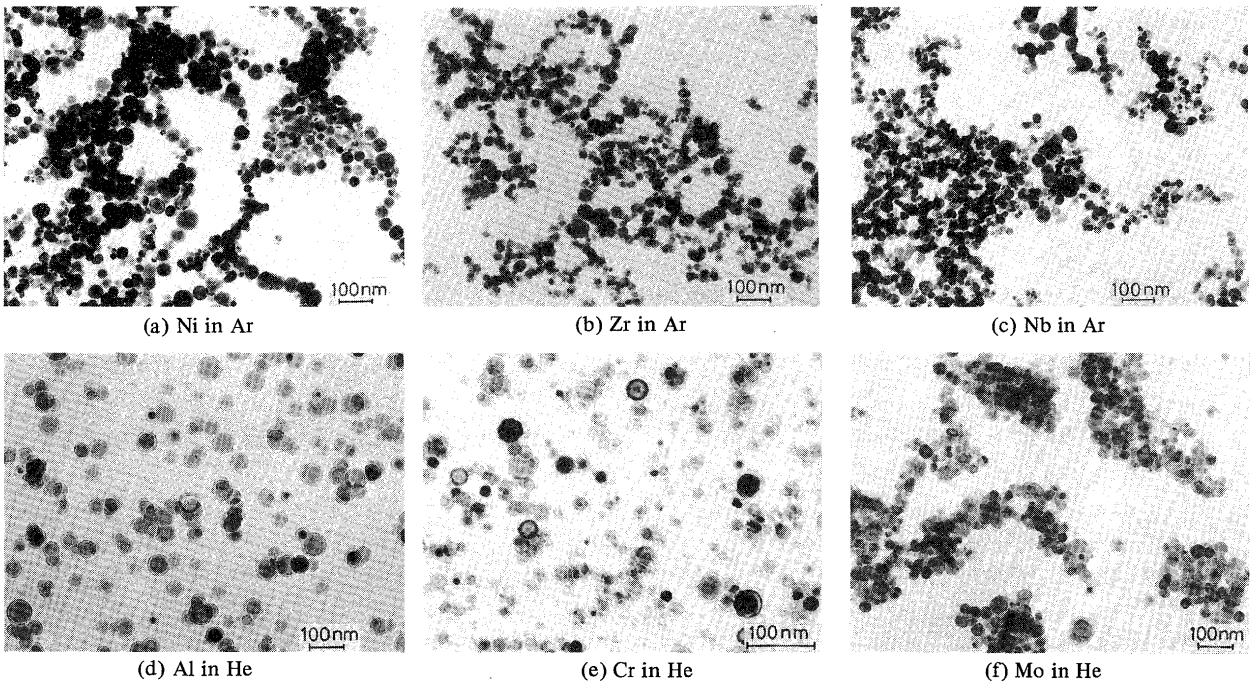

(a) Ni in Ar (b) Zr in Ar (c) Nb in Ar

(d) Al in He (e) Cr in He (f) Mo in He

Fig. 12 TEM photos of Ni (a), Zr (b), Nb (c), Al (d), Cr (e) and Mo (f) ultra-fine particles produced in Ar or He at 0.1 MPa.

phases. In this investigation, δ-Cr phase particles could not be detected by diffraction results although they were reported to be formed by other gas-evaporation techniques using high frequency induction heater or active arc plasma.[1),10)–12)]

In this way metallic ultra-fine particles were produced from other metal sheets in Ar or He atmosphere by laser heating-evaporation process, and these identification results are summarized in **Table 1**. It is noted that any particles produced are uniform in the range of 10 to 30 nm in medium size and less than 100 nm in maximum size and are the phases stable at room temperature except Mn. The color of most ultra-fine powders is black except that Al and Si particles are gray and ocher, respectively.

3.2.2 Influence of ambient pressure on particle sizes

The procedures for controlling the particle sizes and size distribution were further investigated by changing particle-collected locations, laser irradiation conditions, or chamber ambient pressures.

Figure 13 indicates particle size distributions of ultra-fine Ni particles deposited on the glasses. The varied heights of the glasses above the sheet surfaces were 5, 10, 15 and 50 mm and the selected distances from the laser center axis were 3 and 6 mm. The laser irradiation conditions were $E_1 = 22$ J/p and $f_d = 10$ mm. Particles collected were smaller near the laser-irradiated zone and became bigger as the distance was farther. In the cases of more than 15 mm, particles tend to link together and similar size distributions are recognized. This fact suggests that particles are growing bigger rapidly by repeating the collision and incorporation near or just above the evaporation part during laser irradiation.

Subsequently, the influence of laser irradiation conditions was examined at the collection-glass height of 20 mm above the plate surface. As the laser power (energy) density was increased from about 0.9 or 2.1 MW/

Table 1 Summary of characterization (crystal structure, median size, maximum size and color) of ultra-fine particles produced from metal sheets by YAG laser heating-evaporation process in Ar (partly He) atmosphere at 0.1 MPa (1 atm).

Target metals	Fe	Ni	Al	Ti	Zr	Cr	Mo	Ta	Nb
Ultra-fine particles	α-Fe (bcc)	Ni (fcc)	Al (fcc)	α-Ti (hcp)	α-Zr (hcp)	Cr (bcc)	Mo (bcc)	Ta (bcc)	Nb (bcc)
Median size (Max. size)	21 (65)	19 (45)	20 (50)	22 (40)	14 (50)	8 (50)	12 (40)	13 (40)	18 (70)
Powder color	Black	Black	Glay	Black	Black	Black	Black	Black	Black
Target metals	Si	Sn	Pb	Mn	Zn	W	Co	V	Cu
Ultra-fine particles	Si (dia)	β-Sn (tetra)	Pb (fcc)	β-Mn (cubic)	Zn (hcp)	W, (W_3O) (bcc)(β-W)	Co(CoO) (fcc)	V(-) (bcc)	Cu (fcc)
Powder color	Ocher	Black	Black	Black	Black	Black	Black	Black	Black

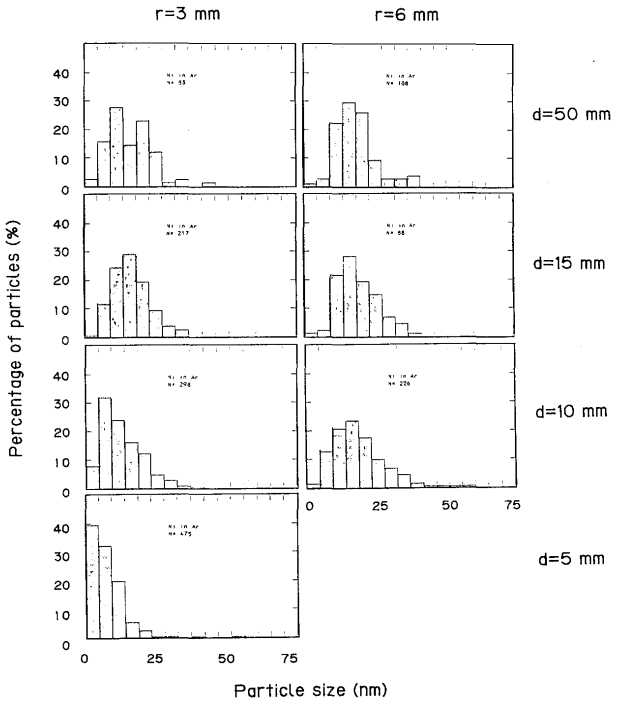

Fig. 13 Comparison of particle size distributions of ultra-fine Ni particles at various collection locations.

cm^2 to 3.1 MW/cm^2 (from 34 or 74 J/mm^2 to 111 J/mm^2), the average particle sizes were decreased from about 19 or 21 nm to 13 nm for Fe, from 15 or 18 nm to 10 nm for Ni, and from 15 or 16 nm to 13 nm for Ti. The sizes of Fe, Ni and Ti particles seemed to decrease slightly as the laser energy or intensity was extremely high (in the case of 20 mm collection-glass height).

Figure 14 (a) to (d) exhibit the TEM photos of ultra-fine Fe particles made at 200 (2 atm), 13.3 (100 torr), 1.3 (10 torr) and 0.1 kPa (about 1 Torr), and their cumulative particl size distributions are compared in **Fig. 15**. It is apparent that the medium size becomes smaller from about 39 nm to 18, 9 and 3 nm and the distribution becomes narrower with a reduction in the pressure from

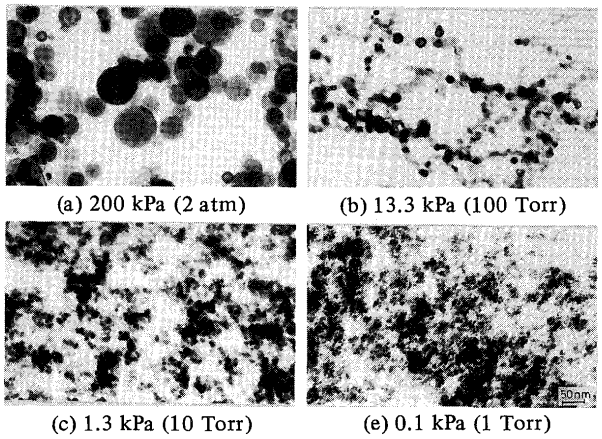

(a) 200 kPa (2 atm) (b) 13.3 kPa (100 Torr)

(c) 1.3 kPa (10 Torr) (e) 0.1 kPa (1 Torr)

Fig. 14 TEM photos of ultra-fine Fe particles produced by laser under Ar pressure of 200 kPa (2 atm) (a), 13.3 kPa (100 torr) (b), 1.3 kPa (10 torr) (c) and 0.1 kPa (1 torr) (d).

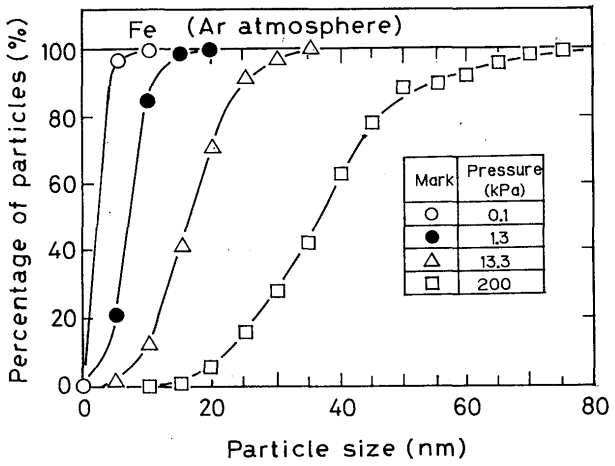

Fig. 15 Cumulative size distribution graph showing comparison of ultra-fine Fe particle sizes made at 0.1, 1.3, 13.3 and 200 kPa.

about 200 to 13.3, 1.3 and 0.1 kPa. As the pressure is decreased, the particle sizes were smaller 37, 20, 17 and 4 nm for Ni and 66, 26, 18 and 4 nm for Ti. The decreases in size with a decrease in the pressure were also confirmed by the diffraction peak broadening of X-ray diffractometer patterns from Fe, Ni and Ti powders. From these results it was found that the decrease in ambient pressure was most beneficial in obtaining much smaller particle sizes and extremely narrower size distribution.

3.3 Laser production of ultra-fine alloy particles

Particles were produced from various Ni-Ti, Fe-Ti and Cu-Ni alloys and Fe-Ti-mixed powders by laser shots in Ar atmosphere at 0.1 to 0.2 MPa (1 to 2 atm) and collected by spray method, and their morphology and particle size distribution were first investigated by TEM observation.

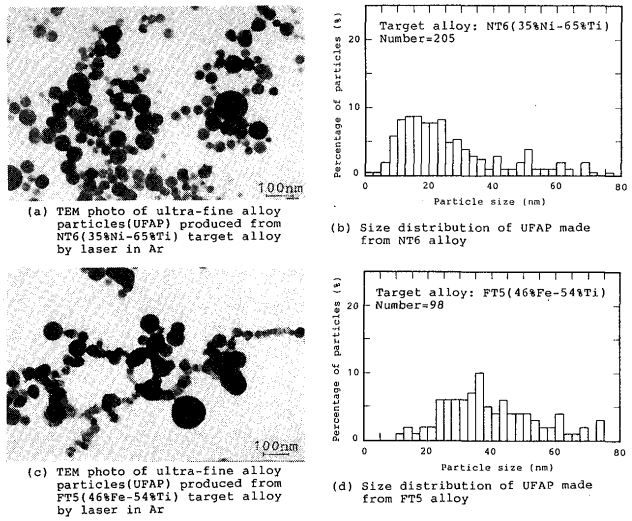

Fig. 16 TEM photos ((a), (c)) and particle size distributions ((b), (d)) of ultra-fine particles produced from NT6 (35%Ni-65%Ti) ((a), (b)) and FT5 (46%Fe-54%Ti) ((c), (d)) target alloys.

Figure 16 (a) to (d) exhibit examples of the TEM photos and particle size distributions of ultra-fine particles produced from NT6 (35%Ni-65%Ti) and FT5 (46%Fe-54%Ti) target alloys. Ultra-fine particles are observed mainly in the projection form of globule, and some particles are linked together like chains. A few particles of about 150 nm maximum diameter are seen, but the great majority of particles are in the narrow size range from 10 to 60 nm.

The compositions of ultra-fine particles deposited on Al plate were analyzed by the EDX of the SEM. **Figure 17** (a), (b) and (c) show the EDX results of FT2 (80%Fe-20%Ti) target alloy, its ultra-fine particles and laser-irradiated fusion zone, respectively. Four peaks of TiK_α (taller), TiK_β (shorter), FeK_α (taller) and FeK_β (shorter) are seen in respective result. By comparison, Ti peaks of ultra-fine particles are shorter and Fe peaks are taller than those of the target alloy, but on the contrary Ti peaks of laser fusion zone are taller than those of the mother alloy. It is deduced from these results that ultra-fine particles of Fe-Ti alloys contain lower Ti contents than their respective target alloys. Thus EDX analyses were further extended to ultra-fine particles produced from other Fe-Ti and Ni-Ti target alloys and Fe-Ti powder mixtures. As a result, the Ti contents of particles were compared with those of Ni-Ti and Fe-Ti target alloys and Fe-Ti powder mixtures in **Fig. 18** (a) and (b). It is clearly understood that ultra-fine particles have lower Ti contents than their target alloys and mixtures. Moreover, the relationship of Cu contents between ultra-fine particles and their Cu-Ni target alloys is shown in **Fig. 19**. Cu-Ni alloy particles with higher Cu content can be produced from their target alloys. Considering that the vaporization temperatures (and heats) of Ti, Fe, Ni and Cu elements are 3533 (8.29), 3273 (6.29), 3003 (6.34) and 2868K (4.29 kJ/g),[15] respectively, the elements with lower vaporization temperatures (and heats) appear to be enriched in alloy particles. In each figure it is also recognized that there is a compositional correlation between particles and target materials, and therefore the compositions of ultra-fine alloy particles are judged to be controllable.

A feasibility of alloy particle formation was examined by X-ray diffractometer method. **Figure 20** shows the results of NT2 (80%Ni-20%Ti) and NT5 (45%Ni-55%Ti) target alloys (upper) and their ultra-fine particles produced (lower), and **Figure 21** indicates the results obtained from FT2 (80%Fe-20%Ti), FT5 (46%Fe-54%Ti) and FT7 (30%Fe-70%Ti) target alloys. In the case of NT2 alloy, Ni_3Ti and partly Ni phases are the constituents of the target alloy, but the crystal structure of ultra-fine particles is Ni phase. NT5 target alloy consists of chiefly $NiTi_2$ and partly NiTi phases, but NiTi phase is the main phase of ultra-fine powders. FT2 target alloy is composed of α-Fe and Fe_2Ti phases, but their ultra-fine particles are

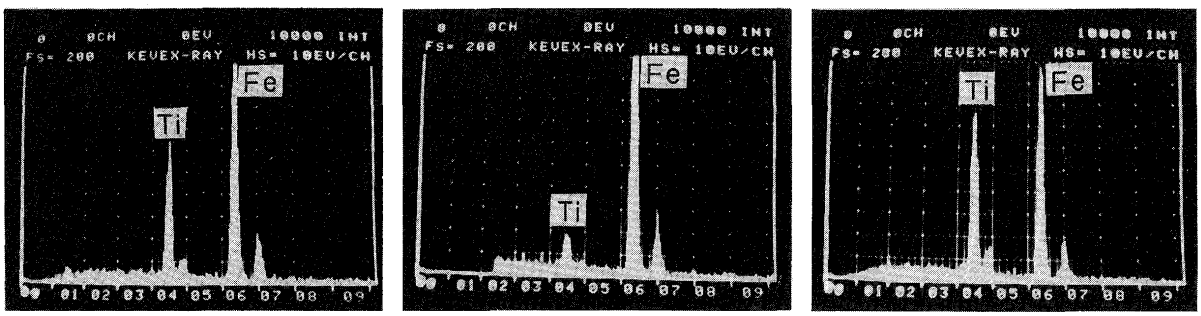

(a) Target alloy before laser shot (b) Ultra-fine particles produced (c) Target alloy (fusion zone) after laser shot

Fig. 17 EDX results of FT2 (80%Fe-20%Ti) target alloy (a), its ultra-fine particles (b) and laser-melted spot (c).

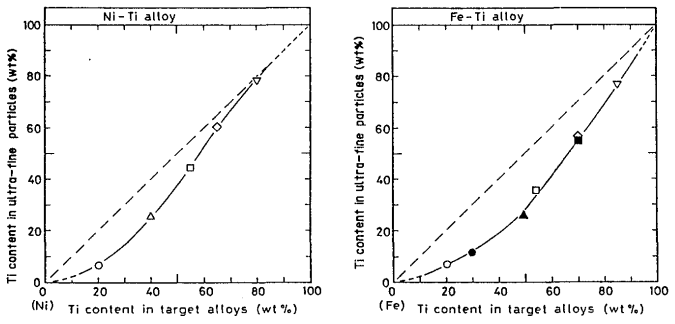

(a) (b)

Fig. 18 Compositional change in Ti content of ultra-fine alloy particles produced from mother targets by laser shot in Ar; (a) Ni-Ti and (b) Fe-Ti alloy systems.

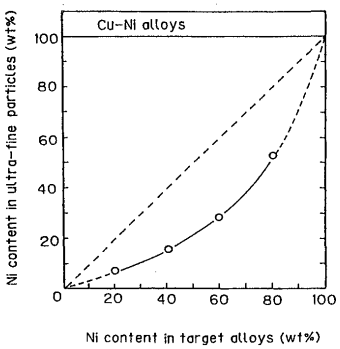

Fig. 19 Relation of Ni contents between ultra-fine Cu-Ni alloy particles produced by laser shots in Ar and their mother Cu-Ni alloy plates.

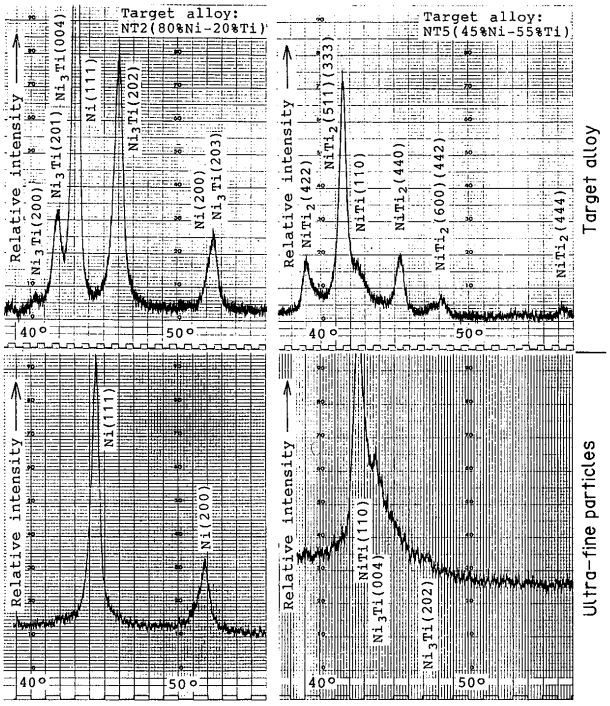

Fig. 20 X-ray diffractometer results of NT2 (80%Ni-20%Ti) and NT5 (45%Ni-55%Ti) target alloys (upper) and their ultra-fine particles produced by irradiating laser in Ar (lower).

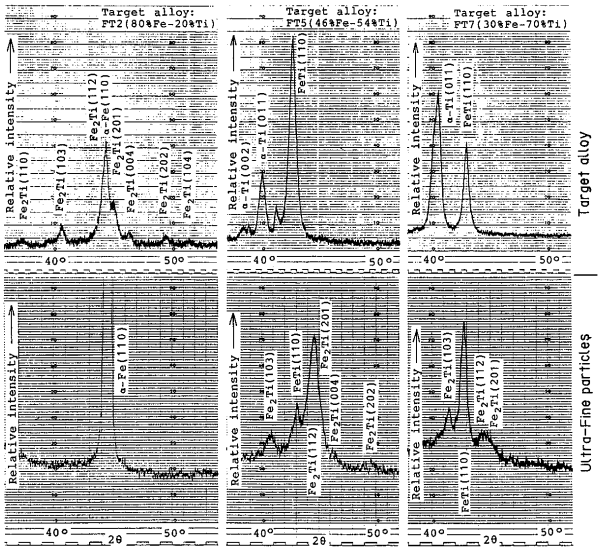

Fig. 21 X-ray diffractometer results of FT2 (80%Fe-20%Ti), FT5 (46%Fe-54%Ti) and FT7 (30%Fe-70%Ti) target alloys and their ultra-fine particles made by laser shots in Ar.

identified as α-Fe phase. The main crystal structures of FT5 and FT7 base metal are α-Ti and FeTi phases, but their particles are predominantly constituted of Fe_2Ti and FeTi phases, respectively. It is found that the particles produced do not necessarily have the same crystal structures as their target alloys, and the main structures of these ultra-fine powders may be interpreted in terms of the compositional deviation that the alloy particles contain lower Ti contents than their Ni-Ti and Fe-Ti target alloys. The results of NT5, FT5 and FT7 target alloys also mean that the laser evaporation process is possible to produce ultra-fine alloy particles of intermetallic compounds.

The compositions and crystal structures of ultra-fine alloy particles produced from Ni-Ti and Fe-Ti target alloys were summarized and tabulated together with those of target alloys in **Tables 2** and **3**. The laser production of ultra-fine alloy particles was comfirmed, and it is understood that the crystal structures of particles are consistent with the phase structures predicted according to the deviated compositions of powders. Besides, the crystal structure of all alloy particles made from Cu-Ni target alloys was fcc α phase of Cu and Ni solid solution.

4. Conclusion

In this study the laser production of various ultra-fine

Table 2 Summary of compositions and constituents of Ni-Ti target alloys and their ultra-fine alloy particles produced by laser shot in Ar.

Target metals (Ni-Ti alloys)	NT2 (80%Ni-20%Ti)	NT4 (60%Ni-40%Ti)	NT5 (45%Ni-55%Ti)	NT6 (35%Ni-65%Ti)	NT8 (20%Ni-80%Ti)
	Ni_3Ti, Ni	NiTi, Ni_3Ti	NiTi, $NiTi_2$	$NiTi_2$, α-Ti	α-Ti, $NiTi_2$
Ultra-fine particles (Composition)	Ni (93%Ni-7%Ti)	NiTi, Ni_3Ti (75%Ni-25%Ti)	NiTi, Ni_3Ti (56%Ni-44%Ti)	$NiTi_2$, NiTi (40%Ni-60%Ti)	α-Ti, $NiTi_2$ (22%Ni-78%Ti)

Table 3 Summary of compositions and constituents of Fe-Ti target alloys and their ultra-fine alloy particles made by laser shot in Ar.

Target metals (Fe-Ti alloys)	FT2 (80%Fe-20%Ti)	FT3 (67%Fe-33%Ti)	FT5 (46%Fe-54%Ti)	FT7 (30%Fe-70%Ti)	FT8 (15%Fe-85%Ti)
	α-Fe, Fe_2Ti	Fe_2Ti, FeTi	FeTi, α-Ti	α-Ti, FeTi	α-Ti
Ultra-fine particles (Composition)	α-Fe (93%Fe-7%Ti)	-- --	Fe_2Ti, FeTi (65%Fe-35%Ti)	FeTi, Fe_2Ti (44%Fe-56%Ti)	α-Ti (24%Fe-76%Ti)

metal and alloy particles were attempted by the pulsed YAG laser heating-vaporization process of target metal and alloy sheets in Ar or He atmosphere. The following main conclusions can be drawn:

(1) Ultra-fine particles were effectively produced under laser irradiation conditions for plume formation, and their production yield was larger at higher laser power densities near the laser conditions for spattering formation.

(2) Ultra-fine particles of Fe, Ni and Ti could be made at extremely high formation rates. On the other hand, the laser production of powders was by far smaller for the metals of great light reflectance, large thermal diffusivity and/or high vaporization temperature.

(3) The formation of ultra-fine particles due to the evaporation phenomenon took place immediately after the onset of laser irradiation and thereafter continued throughout the laser irradiation. These facts meant that the laser energy was efficiently consumed for the evaporation.

(4) The formation and propagation directions of particles were almost perpendicular to the sheet surface and controlled by declining the sheet to the laser axis. This supports that particles could be easily collected in the case of such laser production process.

(5) Ultra-fine metal particles were produced from their own metals in Ar or He at 0.1 MPa (1 atm), and had a median size of about 10 to 30 nm with a maximum size of less than 70 nm.

(6) The majority of particle morphologies of metal particles were spherical or polygonal, and particles of Fe, Cr, Zr and Ta were observed in the projection form of hexagon or octagon.

(7) Most ultra-fine particles are stable phases at room temperature except for Mn powders.

(8) Particle sizes were decreased with a reduction in the ambient pressure. This suggests that particle sizes and their distributions can be easily controlled by regulating the pressure.

(9) The production of ultra-fine alloy particles of less than 150 nm in maximum size was feasible by irradiating a pulsed YAG laser on an alloy or a powder mixture of different metals in Ar atmosphere.

(10) The compositions and crystal structures of ultra-fine alloy particles were judged to be roughly controllable by regulating the compositions of target alloys or the mixture ratio of target powders.

Acknowledgements

The authors wish to thank Mr. M. Tsuchiya, former undergraduate student of Kansai University, for his cooperation in performing some experimental work.

References

1) S. Yatsuya and R. Uyeda: Japanese J. of Applied Physics, Vol. 42 (1973), No. 11, 1067–1085 (in Japanese).

2) S. Kashu: Bul. of The Japan Institute of Metal, Vol. 21 (1982), No. 5, 357–359 (in Japanese).

3) T. Hayashi: Ultra-Fine Particle –Science and Technology–, Japan Chemistry Society, ed., No. 48, 1–211, Gakkai Shuppan Center, (1985) (in Japanese).

4) R. Uyeda: Bul. of The Japan Institute of Metal, Vol. 17 (1978), No. 5, 403–407 (in Japanese).

5) R. Uyeda, et al.: Ultra-Fine Particle, 1–150, Agune Technical Center, (1984) (in Japanese).

6) M. Uda: Bul. of The Japan Institute of Metal, Vol. 22 (1983), No. 5, 412–420 (in Japanese).

7) N. Wada: Japanese J. of Applied Physics, Vol. 50 (1981), No. 2, 151–152 (in Japanese).

8) Y. Saito: Japanese J. of Applied Physics, Vol. 50 (1981), No. 2, 149–150 (in Japanese).

9) N. Wada: Bul. of Ceramic Society of Japan, Vol. 19 (1984), No. 6, 464–471 (in Japanese).

10) S. Ohno and M. Uda: J. of The Japan Institute of Metal, Vol. 48 (1984), 640–646 (in Japanese).

11) M. Uda and S. Ohno: Surface Science, Vol. 5 (1984), No. 4, 426 (in Japanese).

12) M. Uda: J. of The Japan Welding Society, Vol. 54 (1985), No. 6, 318–329 (in Japanese).

13) N. Wada: Japanese J. of Applied Physics, Vol. 5 (1969), 551.

14) N. Wada: Metal, Vol. 48 (1978), 50–56 (in Japanese).

15) S. Iwama and T. Asada: Seimitsukikai (J. of the Japan Society of Precision Engineering), Vol. 48 (1982), No. 2, 248–251 (in Japanese).

16) R. Uyeda, M. Kumazawa, M. Kato, N. Wada and M. Matsumoto: Technical Report of Toyota, Vol. 26 (1973), 66 (in Japanese).

17) M. Kato: Japanese J. of Applied Physics, Vol. 15 (1976), No. 5, 757–760 (in Japanese).

18) S. J. Haggerty and W. R. Cannon: "Laser-Induced Chemical Processes", J. I. Steinfeld, ed., 165–241, Plenum Press, (1981).

19) W. R. Cannon, S. C. Danforth, J. H. Flint, J. S. Haggerty and R. A. Marra: J. Am. Ceram. Soc., Vol. 65 (1982), 324.

20) –News Digests–: Bul. of The Ceramic Society of Japan, Vol. 19 (1984), No. 6, 531 (in Japanese).

21) N. Tabata, H. Nagai, H. Yoshida, M. Hishii, M. Tanaka, Y. Myoi, T. Akiba and T. Takahashi: Proc. of ICALEO'84, –Materials Processing–, Vol. 44 (1984), 238–245.

22) S. Ishida, S. Yoshida, S. Iwama and H. Kimura: Proc. of CLEO, 21–24 May, (1985), Baltimore, Maryland, USA.

23) A. Matsunawa, H. Yoshida and S. Katayama: Proc. of ICALEO '84, J. Mazumder ed., Vol. 44 (1984), 35–42.

24) A. Matsunawa and S. Katayama: Proc. of ICALEO'85, C. Albright ed., (1985), 205–211.

25) A. Matsunawa and S. Katayama: unpublished research performed at JWRI of Osaka Univ.

26) Metals Handbook, Vol. 8, 294, 307, 326, (1973).